

Model-free Change-point Detection using AUC of a Classifier

Rohit Kanrar¹, Feiyu Jiang^{2*}, and Zhanrui Cai^{3*}

¹*Department of Statistics, Iowa State University*

²*School of Management, Fudan University*

³*Faculty of Business and Economics, University of Hong Kong*

Abstract

In contemporary data analysis, it is increasingly common to work with non-stationary complex datasets. These datasets typically extend beyond the classical low-dimensional Euclidean space, making it challenging to detect shifts in their distribution without relying on strong structural assumptions. This paper proposes a novel offline change-point detection method that leverages classifiers developed in the statistics and machine learning community. With suitable data splitting, the test statistic is constructed through sequential computation of the Area Under the Curve (AUC) of a classifier, which is trained on data segments on both ends of the sequence. It is shown that the resulting AUC process attains its maxima at the true change-point location, which facilitates the change-point estimation. The proposed method is characterized by its complete nonparametric nature, significant versatility, considerable flexibility, and absence of stringent assumptions on the underlying data or any distributional shifts. Theoretically, we derive the limiting pivotal distribution of the proposed test statistic under null, as well as the asymptotic behaviors under both local and fixed alternatives. The localization rate of the change-point estimator is also provided. Extensive simulation studies and the analysis of two real-world datasets illustrate the superior performance of our approach compared to existing model-free change-point detection methods.

Key words and phrases: distribution-free, classification, change-point, sample splitting, AUC

*: Corresponding authors.

1 Introduction

In this paper, we focus on detecting distributional changes in a sequence of independent elements $\{\mathbf{Z}_t\}_{t=1}^T$ taking value in a measurable space (E, \mathcal{E}) , which can be formulated as,

$$\begin{aligned} H_0 : \mathbf{Z}_t &\sim \mathcal{P}_X \text{ for all } 1 \leq t \leq T \\ H_1 : \mathbf{Z}_t &\sim \begin{cases} \mathcal{P}_X & \text{for } 1 \leq t \leq t_0 \\ \mathcal{P}_Y & \text{for } t_0 + 1 \leq t \leq T, \end{cases} \quad 1 \leq t_0 < T \text{ is unknown,} \end{aligned} \quad (1.1)$$

where $\mathcal{P}_X \neq \mathcal{P}_Y$ are two unknown distributions. The hypothesis testing problem (1.1) is typically known as the change-point detection problem, with vast literature devoted to this area and broad applications in bioinformatics, climate science, finance, geographic studies, signal processing, and robotics, among many other areas.

Existing change-point detection methods often impose strong structural assumptions regarding the distributions \mathcal{P}_X and \mathcal{P}_Y , and are typically designed for specific scenarios. Most approaches concentrate on either the first- or second-order moments within the classical Euclidean space or rely on parametric assumptions about the data generation process, see, e.g., [Aue and Horváth \(2013\)](#), [Chen and Gupta \(2012\)](#), and [Truong et al. \(2020\)](#) for recent reviews. In recent times, it has become increasingly common to collect data in complex forms, often characterized by high dimensionality and even deviations from the conventional Euclidean space. For instance, financial analysts often encounter high-dimensional stock data to detect distributional shifts during significant economic events like the ‘‘Great Recession’’ ([Chakraborty and Zhang, 2021](#)). In fields such as economic geography, researchers frequently leverage satellite image data to investigate the impact of human activities on various environments ([Atto et al., 2021](#); [Labuzzetta and Zhu, 2024](#)). In urban studies, researchers analyze transportation data for disruptions or changes in traffic patterns ([Chu and Chen, 2019](#)). These examples highlight the formidable challenge of devising a universally applicable change-point detection framework that accommodates diverse data dimensions and types. Given these observations, we propose a novel change-point detection framework named **changeAUC** for detecting general distributional changes, irrespective of data dimensions and types.

1.1 Our Contributions

Our proposed method **changeAUC** is motivated by the recent success of classification algorithms in high-dimensional two-sample testing problems (Kim et al., 2021; Hu and Lei, 2024) and independence testing problems (Cai et al., 2022, 2024). Specifically, **changeAUC** involves a four-step procedure: 1) data-splitting by trimming at the beginning and end of the sequence; 2) training the classifier using splits from beginning and end; 3) recursive splitting of data based on the candidate change-point location; and 4) testing the accuracy of observations in the middle based on AUC, the Area Under the ROC Curve. The key idea behind the classification accuracy test is the following: if the two groups of samples are indeed heterogeneous, a complex classifier should be able to distinguish the underlying distributions, yielding higher accuracy on the test set. We leverage this intuition by training a classifier once, followed by recursively conducting two-sample testing across time points by measuring classification accuracy, thus enabling our objective of change-point detection. The proposed method enjoys several appealing advantages.

- **COMPLETELY NONPARAMETRIC.** It does not impose any parametric assumption on the data distributions. Moreover, it does not impose any structure on the distributional shift, e.g., change occurs in mean or covariance, change is sparse or dense.
- **HIGHLY VERSATILE.** Our approach applies to different data types, encompassing classical low-dimensional Euclidean, high-dimensional, and non-Euclidean data like images and texts. The sole prerequisite is the availability of a suitable classifier.
- **CONSIDERABLY FLEXIBLE.** It can be fine-tuned for any particular application by selecting an appropriate classifier. Such flexibility also enables effective incorporation of prior knowledge into the analysis. For instance, a Convolutional Neural Network (CNN) can identify change-points in images or videos. Our method does not necessitate a consistently accurate classifier. As long as the classifier captures some signals between two distributions, **changeAUC** can effectively detect change-points.

- **DISTRIBUTION-FREE.** Our test statistic has a pivotal limiting distribution under the null. In fact, it is shown to be a functional of Brownian motion, which implies that the critical values can be numerically tabulated.

Rigorous theoretical justifications have been provided to support the good performance of our proposed method. We use empirical process theory (Vaart and Wellner, 2023) to obtain the pivotal limiting distribution of the test statistic under null. The asymptotic behaviors of the test statistic are also derived under local and fixed alternatives. Furthermore, we establish the consistency and localization rate of the maximizer of the AUC process for estimation purposes. Extensive numerical studies on both simulated data and two real applications further corroborate the theoretical findings. The empirical results underscore the effectiveness of our testing framework, demonstrating its ability to control size performance and showcasing competitive power performance compared to existing methods.

1.2 Related Work

The origin of offline change-point problems can be dated back to the seminal work of Page (1954). The classical approaches to tackling change-point problems are typically limited to low dimensional quantities, such as mean and variance, or specific parametric models. We refer to Aue and Horváth (2013), Chen and Gupta (2012), and Truong et al. (2020) for comprehensive reviews. With modern data collection techniques, high-dimensional and non-Euclidean data have become ubiquitous in many scientific areas. In particular, for high dimensional data, extensive works have devoted to mean changes (Jirak, 2015; Cho and Fryzlewicz, 2015; Wang and Samworth, 2018; Enikeeva and Harchaoui, 2019; Yu and Chen, 2020; Wang et al., 2022); covariance changes (Avanesov and Buzun, 2018; Steland, 2019; Dette et al., 2022; Li et al., 2023); and other model parameters (Kaul et al., 2019; Liu et al., 2020). For non-Euclidean data, much effort has been put into Hilbert space, and we mention Berkes et al. (2009); Aue et al. (2018) for functional mean changes and Jiao et al. (2023) for functional covariance changes. We

also note [Dubey and Müller \(2020\)](#) and [Jiang et al. \(2024\)](#) for recent developments in change-point detection of first- and second-order moments for non-Euclidean data in metric space, where classical algebraic operators such as addition and multiplication, do not apply. Previous works primarily focus on detecting only one or two specific types of changes, which may lack power when changes occur in other aspects of data. Nonparametric methods have emerged in recent years as a powerful counterpart to parametric methods for detecting general types of changes. Most methods are appropriate for the low dimensional Euclidean space, see, e.g., [Harchaoui and Cappé \(2007\)](#), [Kawahara and Sugiyama \(2012\)](#), [Liu et al. \(2013\)](#), [Matteson and James \(2014\)](#), [Zou et al. \(2014\)](#), [Arlot et al. \(2019\)](#), [Padilla et al. \(2021\)](#). We are only aware of a few recent developments in high-dimensional data; e.g., [Chakraborty and Zhang \(2021\)](#) utilizes generalized energy distance. However, their method can only capture the pairwise homogeneity (heterogeneity under H_1) of the marginal distributions in high dimensional $(\mathcal{P}_X, \mathcal{P}_Y)$, which may lack power when $(\mathcal{P}_X, \mathcal{P}_Y)$ correspond to the same marginal distributions but differ in other aspects. Some graph-based tests have been proposed recently by [Chen and Zhang \(2015\)](#) and [Chu and Chen \(2019\)](#). Yet, as pointed out by [Chakraborty and Zhang \(2021\)](#), they may lack the power to detect changes in higher-order moments or when the data dimension is high with sparse distributional shifts. In contrast, our proposed approach takes advantage of contemporary classifiers within the statistics and machine learning community. This adaptability allows us to detect changes beyond marginal distributions and moments, setting our method apart in terms of its capability to uncover variations in high-dimensional data and even non-Euclidean data. These findings are further corroborated by simulation studies in [Section 4](#).

We also mention a few recent contributions that borrow the strength of classifiers in the context of two-sample testing and change-point problems. Since [Kim et al. \(2021\)](#), there has been a flurry of efforts that employ classifiers to conduct two-sample tests, see, e.g., [Lopez-Paz and Oquab \(2016\)](#), [Kim et al. \(2019\)](#), [Kirchler et al. \(2020\)](#). However, the extension to the change-point context seems largely unexplored, except for [Lee et al. \(2023\)](#), [Wang et al. \(2023\)](#),

Londschien et al. (2023), and Li et al. (2024). In particular, for online data, both Lee et al. (2023) and Wang et al. (2023) leverage neural networks to estimate likelihood ratio functions for change-point detection. For offline data, Londschien et al. (2023) employs the random forest classifier for detecting change-points by introducing a classifier-based nonparametric likelihood ratio, while Li et al. (2024) proposes to use neural networks for detecting change-points in time series under supervised setting. Compared with offline methods, our proposed framework differs in several key aspects. 1) Both of the aforementioned methods implicitly assume Euclidean data type, whereas our approach additionally accommodates non-Euclidean data with appropriate classifiers. 2) Neither of the aforementioned methods offers asymptotic results, leading to increased computational demands through permutation or conservative type-I error controls. In contrast, our method offers an asymptotic approach by providing a pivotal limiting null distribution, facilitating practical statistical inference. Therefore, our results complement their works, particularly in the theoretical aspect. 3) Unlike the nonparametric likelihood used by Londschien et al. (2023) and the empirical risk minimizer-based classification accuracy utilized by Li et al. (2024), we measure classification accuracy using the AUC. Compared with likelihood-ratio-based methods, which can be difficult to compute in high-dimensional settings or when specifying the likelihood is challenging, the use of AUC from a classifier offers greater robustness by relieving reliance on specific distributional assumptions. In addition, the rank-sum comparison in AUC provides robustness against estimation error of likelihood ratio and classification probability, meaning that the classifier does not need to be strictly consistent. It allows for weakly trained classifiers without extensive hyperparameter tuning. More discussions are deferred to Section 2. Lastly, we mention a similar data-splitting approach implemented by Gao et al. (2023), where the authors propose a dimension-agnostic change-point test statistic by projecting middle observations to the direction determined by observations at both ends of the sequence. However, it is designed only for detecting a change in the mean, while our method is more general and uses rank-sum comparison through AUC.

The rest of this article is organized as follows. Section 2 introduces our proposed method with comprehensive justifications for each step. Theoretical analysis is conducted in Section 3. Section 4 showcases the finite sample performance of our framework. Section 5 demonstrates the application of our method to two real datasets. Section 6 concludes with discussions and future directions. All technical proofs are deferred to the Appendix.

2 Methods

Section 2.1 outlines **changeAUC** for detecting at most one change-point in a sequence of independent observations. Section 2.2 provides a detailed justification of the steps of our proposed framework. Section 2.3 extends the method to estimate multiple change-points.

2.1 Proposed Method

Consider a sequence of independent random elements $\{\mathbf{Z}_t\}_{t=1}^T$ defined on a common probability space $(\Omega, \mathcal{F}, \mathbb{P})$ and taking value in a measurable space (E, \mathcal{E}) . Let \mathcal{P}_X and \mathcal{P}_Y be two different probability distributions on the same probability space such that $\mathcal{P}_X, \mathcal{P}_Y$ are absolutely continuous with respect to each other, i.e., $\mathcal{P}_X \ll \mathcal{P}_Y$ and $\mathcal{P}_Y \ll \mathcal{P}_X$. To test (1.1), our proposed methodology consists of the following four steps:

1. **Sample Splitting:** For a small trimming parameter $\epsilon \in (0, 1/2)$ with $m = \lfloor T\epsilon \rfloor$, data are split into three parts: $D_0 \stackrel{\text{def}}{=} \{\mathbf{Z}_t\}_{t=1}^m$, $D^v \stackrel{\text{def}}{=} \{\mathbf{Z}_t\}_{t=m+1}^{T-m}$ and $D_1 \stackrel{\text{def}}{=} \{\mathbf{Z}_t\}_{t=T-m+1}^T$.
2. **Training Classifier:** Labels $v_t = 0$ for $\mathbf{Z}_t \in D_0$ and $v_t = 1$ for $\mathbf{Z}_t \in D_1$ are assigned and a classifier is trained based on observations from beginning and end of the sequence, i.e., $\{(v_t, \mathbf{Z}_t) : \mathbf{Z}_t \in D_0 \cup D_1\}$.

For steps below, let $\hat{\theta}(\cdot)$ be the estimated conditional probability distribution associated with the classifier. Given a new observation $\mathbf{Z} = \mathbf{z} \in E$, $\hat{\theta}(\mathbf{z}) = \hat{\mathbb{P}}[v = 1 | \mathbf{Z} = \mathbf{z}]$ is the estimated probability of $\mathbf{Z} = \mathbf{z}$ being generated by the same distribution as D_1 .

3. **Recursive Splitting:** For another small trimming parameter $\eta \in (0, 1/2 - \epsilon)$ and the set of candidate change-points $\mathcal{I}_{cp} \stackrel{\text{def}}{=} \{\lfloor Tr \rfloor : r \in [\epsilon + \eta, 1 - \epsilon - \eta]\}$, validation data D^v are split into two parts for each $k \in \mathcal{I}_{cp}$: $D_0^v(k) \stackrel{\text{def}}{=} \{\mathbf{Z}_t\}_{t=m+1}^k$ and $D_1^v(k) \stackrel{\text{def}}{=} \{\mathbf{Z}_t\}_{t=k+1}^{T-m}$.
4. **Measuring Accuracy:** For each $k \in \mathcal{I}_{cp}$, labels $v_t = 0$ for all $\mathbf{Z}_t \in D_0^v(k)$ and $v_t = 1$ for all $\mathbf{Z}_t \in D_1^v(k)$ are assigned to calculate the Area Under the Receiver Operating Characteristic (ROC) curve (AUC) using $\{(v_t, \mathbf{Z}_t) : \mathbf{Z}_t \in D_0^v(k) \cup D_1^v(k)\}$:

$$\widehat{\Psi}(k) \stackrel{\text{def}}{=} \frac{1}{(k-m)(T-m-k)} \sum_{i=m+1}^k \sum_{j=k+1}^{T-m} \mathbb{I}\{\widehat{\theta}(\mathbf{Z}_i) < \widehat{\theta}(\mathbf{Z}_j)\}.$$

Above four steps are repeated for all candidate change-points to obtain AUCs, $\{\widehat{\Psi}(k)\}_{k \in \mathcal{I}_{cp}}$.

Remark 1. *The choices of ϵ and η are subjective. A moderate value of $m = \lfloor T\epsilon \rfloor$ is essential for appropriate classifier training. A smaller choice of ϵ may result in power loss, whereas a larger ϵ requires the change-point to exist in the middle of the sequence. In practice, we propose to fix $\epsilon = 0.15$. However, choosing a smaller ϵ in our framework is feasible, particularly when the sample size is substantial or if the classification algorithm performs well with a smaller training sample. Notably, under the supervised setting or when knowledge transfer is plausible through a pre-trained classifier, a much smaller value of ϵ is allowed. The role of η works as the trimming parameter commonly adopted in change-point literature, see [Andrews \(1993\)](#). We propose to fix $\eta = 0.05$ for practical implementations.*

Under H_0 with no change-point, $\widehat{\Psi}(k)$ is expected to be close to 0.5 for all values of k , resembling a random guess. In contrast, under H_1 , $\widehat{\Psi}(k)$ is anticipated to exceed 0.5 for k near the true change-point t_0 , allowing for differentiation between the two distributions. Therefore, the test statistic is formulated by choosing the maximal AUC,

$$\widehat{Q}_T \stackrel{\text{def}}{=} \max_{k \in \mathcal{I}_{cp}} \widehat{\Psi}(k).$$

The resulting maximizer, $\widehat{R}_T \stackrel{\text{def}}{=} \operatorname{argmax}_{k \in \mathcal{I}_{cp}} \widehat{\Psi}(k)$, is then used for change-point estimation. We expect to find more evidence against H_0 in (1.1) for a large value of \widehat{Q}_T . Section 3 rigorously

investigates the asymptotic behavior of \widehat{Q}_T under the null hypothesis H_0 and establishes that, after appropriate scaling, it converges weakly to a pivotal process:

$$\sup_{k \in \mathcal{I}_{cp}} \left\{ \sqrt{T}(\widehat{\Psi}(k) - 1/2) \right\} \xrightarrow{d} \sup_{r \in [\gamma, 1-\gamma]} G_0(r) \quad \text{as } T \rightarrow \infty, \quad (2.1)$$

where $\gamma \stackrel{\text{def}}{=} \epsilon + \eta$, and $G_0(\cdot)$ is a pivotal functional of standard Brownian motions. Therefore, we can simulate the theoretical quantiles and devise a test for H_0 . Specifically, we generate 10^5 i.i.d. standard normal random variables to approximate one realization of the standard Brownian motion path. Let $Q(1 - \alpha)$ be the $100(1 - \alpha)\%$ quantile of $\sup_{r \in [\gamma, 1-\gamma]} G_0(r)$. Based on 10^5 Monte Carlo simulations, Table 1 outline the value of $Q(1 - \alpha)$ for $\alpha = 20\%, 10\%, 5\%, 1\%$ and 0.5% respectively. Consequently, a level- α test for detecting a single change-point rejects H_0 if $\sqrt{T}(\widehat{Q}_T - 1/2) \geq Q(1 - \alpha)$. A comprehensive view of steps involved in **changeAUC** is presented in Algorithm 1.

Table 1: Simulated quantiles of $\sup_{r \in [\gamma, 1-\gamma]} G_0(r)$ for $\gamma = \epsilon + \eta, \epsilon = 0.15, \eta = 0.05$.

α	20%	10%	5%	1%	0.5%
$Q(1 - \alpha)$	2.231	2.664	3.040	3.784	4.051

2.2 Classification Accuracy for Detecting a Single Change-point

In practice, both $\mathcal{P}_X, \mathcal{P}_Y$ and t_0 are unknown. To test (1.1), it is important to distinguish \mathcal{P}_Y from \mathcal{P}_X . The fundamental feature of **changeAUC** lies in training an appropriate classifier to discern the heterogeneity between the two unknown distributions. Let $\theta(\cdot)$ be the true conditional probability corresponding to $\widehat{\theta}(\cdot)$. When infinite samples are drawn from two distributions, \mathcal{P}_X and \mathcal{P}_Y , and each sample is associated with a label $v = 0$ or $v = 1$ depending on its origin, we obtain the true conditional probability, $\theta(\mathbf{z}) \stackrel{\text{def}}{=} \mathbb{P}[v = 1 | \mathbf{Z} = \mathbf{z}]$ where $\mathbf{Z} = \mathbf{z} \in E$ is a new observation. Moreover, $\theta(\cdot)$ is related to the true likelihood ratio,

$$L(\mathbf{z}) \stackrel{\text{def}}{=} \frac{\theta(\mathbf{z})}{1 - \theta(\mathbf{z})} = \frac{d\mathcal{P}_Y}{d\mathcal{P}_X}(\mathbf{z}), \quad (2.2)$$

Algorithm 1 changeAUC: single change-point detection.

Require: Data $\{\mathbf{Z}_t\}_{t=1}^T$; choice of classifier; choices of tuning parameters, $\epsilon \in (0, 1/2)$ and

$\eta \in (0, 1/2 - \epsilon)$; significance level α .

1: Split the data into D_0, D^v, D_1 using $m = \lfloor T\epsilon \rfloor$ and obtain \mathcal{I}_{cp} from D^v using η .

2: Train the classifier based on D_0, D_1 to obtain $\{\hat{\theta}(\mathbf{Z}_t) : \mathbf{Z}_t \in D^v\}$.

3: **for** $k \in \mathcal{I}_{cp}$ **do**

4: Split D^v into $D_0^v(k), D_1^v(k)$.

5: Calculate $\hat{\Psi}(k)$, based on $\{\hat{\theta}(\mathbf{Z}_t) : \mathbf{Z}_t \in D_0^v(k)\}$ and $\{\hat{\theta}(\mathbf{Z}_t) : \mathbf{Z}_t \in D_1^v(k)\}$.

6: **end for**

7: Compute $\hat{Q}_T \stackrel{\text{def}}{=} \max_{k \in \mathcal{I}_{cp}} \hat{\Psi}(k)$ and $\hat{R}_T \stackrel{\text{def}}{=} \operatorname{argmax}_{k \in \mathcal{I}_{cp}} \hat{\Psi}(k)$.

8: **if** $\sqrt{T}(\hat{Q}_T - 1/2) > Q(1 - \alpha)$ **then**

9: **return** \hat{R}_T as a significant change-point

10: **end if**

and $L(\mathbf{z}) = 1$ almost surely if $\mathcal{P}_X = \mathcal{P}_Y$. Otherwise, $L(\mathbf{z})$ is expected to be larger (smaller) than one if $\mathbf{Z} \sim \mathcal{P}_Y$ ($\mathbf{Z} \sim \mathcal{P}_X$), respectively. Therefore, $L(\mathbf{z})$, or equivalently $\theta(\mathbf{z})$, serves as a one-dimensional projection of the original observation \mathbf{z} . Proposition 1 below states the close relationship between such projection and the total variation between two distributions. It provides an initial motivation for employing a rank-sum comparison of $L(\cdot)$.

Proposition 1. *For two probability measures \mathcal{P}_X and \mathcal{P}_Y on a common probability space $(\Omega, \mathcal{F}, \mathbb{P})$ such that $\mathcal{P}_Y \ll \mathcal{P}_X$, with the Radon-Nikodyn derivative $d\mathcal{P}_Y/d\mathcal{P}_X(\cdot)$ having a continuous distribution under \mathcal{P}_X , let $\mathbf{Z}_X \sim \mathcal{P}_X$ and $\mathbf{Z}_Y \sim \mathcal{P}_Y$ be independent. Then,*

$$\frac{1}{2}d_{tv}(\mathcal{P}_X, \mathcal{P}_Y) \leq \mathbb{P} \left\{ \frac{d\mathcal{P}_Y}{d\mathcal{P}_X}(\mathbf{Z}_X) < \frac{d\mathcal{P}_Y}{d\mathcal{P}_X}(\mathbf{Z}_Y) \right\} - \frac{1}{2} \leq d_{tv}(\mathcal{P}_X, \mathcal{P}_Y), \quad (2.3)$$

where, $d_{tv}(\mathcal{P}_X, \mathcal{P}_Y)$ is the total variation distance between \mathcal{P}_X and \mathcal{P}_Y .

Given a large total variation distance between the two probability distributions, we expect that an empirical estimate of the probability in (2.3) will capture the heterogeneity between \mathcal{P}_X and \mathcal{P}_Y . Note that the probability in (2.3) involves a rank comparison of the likelihood ratio,

$L(\cdot) \stackrel{\text{def}}{=} (d\mathcal{P}_Y/d\mathcal{P}_X)(\cdot)$. For low-dimensional Euclidean data, it is common to estimate \mathcal{P}_Y and \mathcal{P}_X directly, see e.g. [Padilla et al. \(2021\)](#). However, for high-dimensional Euclidean data, direct estimation of the individual likelihood functions is challenging and usually inconsistent due to the curse of dimensionality. Instead, it is possible to approximate the likelihood ratio $L(\cdot)$ by plugging a surrogate estimator $\widehat{\theta}(\cdot)$ in (2.2):

$$\widehat{L}(\mathbf{z}) \stackrel{\text{def}}{=} \frac{\widehat{d\mathcal{P}_Y}}{d\mathcal{P}_X}(\mathbf{z}) = \frac{\widehat{\theta}(\mathbf{z})}{1 - \widehat{\theta}(\mathbf{z})}. \quad (2.4)$$

The two-sample rank-sum comparison of $\widehat{L}(\mathbf{z})$ is equivalent to the AUC ([Fawcett, 2006](#); [Chakravarti et al., 2023](#)). Specifically, for each change-point candidate k , based on the validation data $D_0^v(k)$ and $D_1^v(k)$, provided $\widehat{\theta}(\mathbf{Z}_t) \in (0, 1) \forall t = m+1, \dots, T-m$, we have

$$\begin{aligned} \widehat{\Psi}(k) &\stackrel{\text{def}}{=} \frac{1}{(k-m)(T-m-k)} \sum_{i=m+1}^k \sum_{j=k+1}^{T-m} \mathbb{I} \left\{ \widehat{\theta}(\mathbf{Z}_i) < \widehat{\theta}(\mathbf{Z}_j) \right\} \\ &= \frac{1}{(k-m)(T-m-k)} \sum_{i=m+1}^k \sum_{j=k+1}^{T-m} \mathbb{I} \left\{ \frac{\widehat{\theta}(\mathbf{Z}_i)}{1 - \widehat{\theta}(\mathbf{Z}_i)} < \frac{\widehat{\theta}(\mathbf{Z}_j)}{1 - \widehat{\theta}(\mathbf{Z}_j)} \right\} \\ &= \frac{1}{(k-m)(T-m-k)} \sum_{i=m+1}^k \sum_{j=k+1}^{T-m} \mathbb{I} \left\{ \widehat{L}(\mathbf{Z}_i) < \widehat{L}(\mathbf{Z}_j) \right\}, \end{aligned} \quad (2.5)$$

where, the second equality holds since, $x \rightarrow x/(1-x)$ is a monotone transformation for $x \in (0, 1)$. Intuitively, if k is indeed a change-point, $\Psi(k)$ can be viewed as an empirical estimator of $\mathbb{P} \{d\mathcal{P}_Y/d\mathcal{P}_X(\mathbf{Z}_X) < d\mathcal{P}_Y/d\mathcal{P}_X(\mathbf{Z}_Y)\}$ based on a second-order U-statistic. Therefore, the AUC-based test can be regarded as an alternative approximation to the likelihood-ratio-based test. Indeed, there is another line of research that directly targets the likelihood ratio, such as in [Kawahara and Sugiyama \(2012\)](#), [Liu et al. \(2013\)](#), and [Wang et al. \(2023\)](#). However, these methods still rely on specifying a model structure for the likelihood ratios, which may be susceptible to systematic bias. On the contrary, our methods rely on ranks instead of explicit likelihood values or ratios, offering greater robustness to distributional assumptions. For instance, our approach remains effective even when $\widehat{L}(\cdot)$ is estimated with bias or is proportional to some unknown constant. This makes it more advantageous when the true data distribution is complex or when

specifying the likelihood (ratio) is challenging. Furthermore, the rank-sum comparison also allows the incorporation of weakly trained classifiers. We include more discussion on this direction in Remark 2.

Remark 2. *Compared with methods using exact values of estimated (conditional) probabilities $\hat{\theta}(\mathbf{Z}_t)$'s, the AUC-based test evaluates the (conditional) rank order of the data rather than relying on these exact values, making it less sensitive to estimation errors due to sample splitting. This is corroborated in Section 4.2 where directly using outputs of the classifier within the CUSUM statistic can lead to distorted type-I error control. In the case of a single change-point at t_0 , estimation is achieved when the sets of conditional probabilities, $\{\hat{\theta}(\mathbf{Z}_t) : \mathbf{Z}_t \in D_0^v\}$ and $\{\hat{\theta}(\mathbf{Z}_t) : \mathbf{Z}_t \in D_1^v\}$ are well separated. Unlike approaches requiring these sets to be close to 0 and 1, respectively, as typically obtained through training a consistent classifier, our framework exhibits robust performance even when such conditions are not strictly met. In particular, Section 3 below highlights that the use of rank-sum comparison alleviates the necessity for a consistently estimated $\hat{\theta}(\cdot)$.*

2.3 Extension to Multiple Change-points

It is feasible to integrate **changeAUC** into existing algorithms designed for estimating multiple change-points, such as wild binary segmentation (Fryzlewicz, 2014), seeded binary segmentation (SBS) (Kovács et al., 2023), isolating single change-points (Anastasiou and Fryzlewicz, 2022), among others. In this paper, we employ the SBS to estimate multiple change-points in two real datasets in Section 5. The SBS procedure works as follows. For a sequence of length T , the SBS recursively applies a single change-point test statistic such as ours to a set of predetermined intervals \mathcal{I}_λ defined as:

$$\mathcal{I}_\lambda = \bigcup_{k=1}^{\lceil \log_{1/\gamma}(T) \rceil} \mathcal{I}_k, \quad \mathcal{I}_k = \bigcup_{i=1}^{T_k} \{(\lfloor (i-1)s_k \rfloor, \lfloor (i-1)s_k + l_k \rfloor)\}, \quad (2.6)$$

where $\lambda \in [1/2, 1)$ is known as a decay parameter, and each \mathcal{I}_k is a collection of sub-intervals of length $l_k = T\gamma^{k-1}$ evenly shifted by $s_k = (T - l_k)/(T_k - 1)$. The SBS finds the largest value

of test statistics evaluated at all sub-intervals and compares it with a predetermined threshold level Δ . Once the maximum test statistic exceeds Δ , a change-point is claimed. The data are further divided into two sub-samples accordingly, and the same procedure is applied to each sub-samples. [Kovács et al. \(2023\)](#) specifically addresses multiple change-point detection in the mean only. Their threshold Δ may not be directly applicable when integrating **changeAUC** into their algorithm, necessitating new theoretical developments for overall control of type-I error in the presence of multiple change-points beyond the mean of distributions. We defer this aspect to future work. Instead, we follow the approach proposed by [Dubey and Zheng \(2023\)](#) and perform a permutation test to obtain the threshold Δ . Algorithm 2 outlines the procedure for this approach. In practice, Δ is set to be the 90% quantile of the permutation null distribution of the maximal test statistics, and $\gamma = 1/\sqrt{2}$.

3 Theoretical Justification

In this section, we investigate the theoretical properties of **changeAUC**. Section 3.1 derives the limiting null distribution of the test statistic, which justifies our claims in (2.1). Section 3.2 investigates the power behavior under fixed and local alternatives. Section 3.3 presents the consistency property of the change-point estimator \hat{R}_T . In what follows, \mathbb{P}_* , \mathbb{E}_* , Var_* and, Cov_* respectively denote the conditional probability, expectation, variance, and covariance given the trained classifier and the training data $D_0 \cup D_1$.

3.1 Limiting Null Distribution

Recall that $\hat{Q}_T \stackrel{\text{def}}{=} \max_{k \in \mathcal{I}_{cp}} \hat{\Psi}(k)$ is the proposed statistic for testing H_0 vs H_1 . With suitable scaling, it is customary to study the limiting behavior of the AUC process: $\{\hat{\Psi}(\lfloor Tr \rfloor)\}_{r \in [\gamma, 1-\gamma]}$, where $\gamma \stackrel{\text{def}}{=} \epsilon + \eta$. In Theorem 1, we show that $\{\sqrt{T}(\hat{\Psi}(\lfloor Tr \rfloor) - 1/2)\}_{r \in [\gamma, 1-\gamma]}$ converges uniformly to a pivotal process with respect to the conditional probability measure \mathbb{P}_* .

Algorithm 2 changeAUC-SBS: multiple change-points detection.

Require: l and u : lower and upper boundaries of time index; all parameters of **changeAUC** in Algorithm 1, minLen : minimum length of intervals, γ : decay parameter, $\hat{\tau}$: initial set of change-points, B : number of permutations.

```

1: procedure CHANGEAUC-SBS( $l, u, \gamma, \hat{\tau}, \text{minLen}$ )
2:   if  $u - l < \text{minLen}$  then
3:     STOP
4:   else
5:     calculate seeded intervals  $\mathcal{I}_\lambda = \{[l_i, u_i] : i \in |\mathcal{I}_\lambda|\}$ .
6:     for  $i = 1, \dots, |\mathcal{I}_\lambda|$  do
7:       Apply changeAUC on  $\{\mathbf{z}_t : t \in [l_i, u_i] \cap \mathbb{N}\}$ .
8:       Denote the maximum AUC as  $\hat{Q}_i$  and maximizer as  $\hat{R}_i$ .
9:     end for
10:    for  $b = 1, \dots, B$  do
11:      Permute  $\{\mathbf{z}_t : t \in [l, u] \cap \mathbb{N}\}$ . Apply changeAUC on the permuted sample.
12:      Denote  $\hat{Q}^{(b)}$  as the maximum AUC.
13:    end for
14:    Calculate  $\Delta$ : 90% quantile of  $\{\hat{Q}^{(b)}\}_{b=1}^B$ .
15:    if  $\max_{i \in \{1, \dots, |\mathcal{I}_\lambda|\}} \hat{Q}_i \geq \Delta$  then
16:      Fix  $m_Q = \arg\max_{i \in \{1, \dots, |\mathcal{I}_\lambda|\}} \hat{Q}_i$  and  $\hat{\tau} = \hat{\tau} \cup \hat{R}_{m_Q}$ 
17:      Implement changeAUC-SBS( $l, \hat{R}_{m_Q}, \gamma, \hat{\tau}, \text{minLen}$ ).
18:      Implement changeAUC-SBS( $\hat{R}_{m_Q} + 1, u, \gamma, \hat{\tau}, \text{minLen}$ ).
19:    else
20:      break
21:    end if
22:  end if
  return  $\hat{\tau}$ : final set of change-points.
23: end procedure

```

Theorem 1. Suppose $\widehat{\theta}(z)$ is continuous with respect to \mathcal{P}_X . Then, under H_0 , it follows that,

$$\left\{ \sqrt{T} \left(\widehat{\Psi}(\lfloor Tr \rfloor) - 1/2 \right) \right\}_{r \in [\gamma, 1-\gamma]} \overset{d}{\rightsquigarrow} \{G_0(r)\}_{r \in [\gamma, 1-\gamma]}, \quad \text{in } L^\infty([0, 1]),$$

under \mathbb{P}_* , where for a standard Brownian Motion (BM) $B(\cdot)$, $G_0(\cdot)$ is defined as

$$G_0(r) \stackrel{\text{def}}{=} \frac{1}{\sqrt{12}} \left[\frac{B(1-\epsilon) - B(r)}{1-\epsilon-r} - \frac{B(r) - B(\epsilon)}{r-\epsilon} \right], \quad \text{for } r \in [\gamma, 1-\gamma]. \quad (3.1)$$

Here, $G_0(r)$ is a functional of standard BM that does not depend on the classifier, data dimension, or data distribution. Theorem 1 leads us to propose a computationally feasible yet statistically sound testing framework using simulated theoretical quantiles in Table 1.

In Theorem 1, we do not require that $\widehat{\theta}(\cdot)$ is consistently estimated. In fact, under H_0 , a random guess is also applicable. The key assumption lies in the continuity of $\widehat{\theta}(\cdot)$ with respect to \mathcal{P}_X , which is typically satisfied for commonly used classifiers such as logistic regression, random forest, and deep neural networks. When there exists a point mass, we can inject a random tie-breaking ranking scheme, and all the theory still goes through.

Remark 3. Throughout the paper, we assume temporal independence among data. While this assumption simplifies the analysis, we briefly discuss how our methodology and theory could be extended to accommodate the time series setting. First, the independence assumption ensures a unified constant variance ($1/12$ appeared in $G_0(r)$) for the rank-sum statistics under H_0 . For time series data, however, a (long-run) variance estimator is required and typically involves additional tuning parameters, such as the bandwidth of a kernel function. In such cases, a self-normalization (Zhao et al., 2022) technique can be employed to mitigate these challenges. Second, we may require additional trimming parameters to control for the serial dependence of D^v on $D_0 \cup D_1$; see similar treatments in Gao et al. (2023). Otherwise, the estimated classifier $\widehat{\theta}(\cdot)$ is correlated with $\mathbf{Z}_t \in D^v$, which greatly complicates the theoretical analysis. Note in the independent setting, this issue is automatically resolved. Third, the concentration inequalities and empirical process theory developed in this paper must be modified accordingly to account for temporal dependence. This is left for future research.

3.2 Uniform Weak Convergence Under Local and Fixed Alternative

Next, we investigate the limiting behaviors of the test under the alternative hypothesis of at most one change-point. Let the true change-point be $t_0 = \lfloor \tau T \rfloor$ for some $\tau \in [\gamma, 1 - \gamma]$. The observations are generated from the following setup:

$$\mathbf{Z}_t \stackrel{\text{iid}}{\sim} \begin{cases} \mathcal{P}_X & \text{for } 1 \leq t \leq t_0 \\ \mathcal{P}_Y & \text{for } t_0 + 1 \leq t \leq T. \end{cases}$$

Let us recall the likelihood ratio, $L(\cdot) = (d\mathcal{P}_Y/d\mathcal{P}_X)(\cdot)$ from (2.2). The following proposition quantifies how it is connected to the total variation distance between \mathcal{P}_X and \mathcal{P}_Y and thus the departure of H_1 from H_0 .

Proposition 2. *Consider two probability measures \mathcal{P}_X and \mathcal{P}_Y that satisfy the conditions in Proposition 1. Let $\mathbf{Z}_X, \mathbf{Z}'_X \stackrel{\text{iid}}{\sim} \mathcal{P}_X$ be independent random elements, and define*

$$\delta \stackrel{\text{def}}{=} \mathbb{E} |L(\mathbf{Z}_X) - L(\mathbf{Z}'_X)|, \quad \text{for } \mathbf{Z}_X, \mathbf{Z}'_X \stackrel{\text{iid}}{\sim} \mathcal{P}_X. \quad (3.2)$$

Then, for the total variation distance $d_{tv}(\mathcal{P}_X, \mathcal{P}_Y)$ between \mathcal{P}_X and \mathcal{P}_Y , we have

$$2d_{tv}(\mathcal{P}_X, \mathcal{P}_Y) \leq \delta \leq 4d_{tv}(\mathcal{P}_X, \mathcal{P}_Y).$$

Note that $\delta = 0$ if and only if $L(\cdot)$ is a constant measurable function, which is equivalent to $\mathcal{P}_X \equiv \mathcal{P}_Y$ almost surely. Therefore, δ can measure how much the alternative hypothesis H_1 deviates from the null hypothesis H_0 .

To facilitate the analysis of power behavior, we let $\delta = \delta_T \geq 0$ that allows the signal to be changing with the sample size. In Section 3.2.1, we present the limiting behavior of \hat{Q}_T under the fixed alternative framework $\sqrt{T}\delta_T \rightarrow \infty$. Section 3.2.2 investigates the limiting behavior of \hat{Q}_T , under a local alternative framework $\sqrt{T}\delta_T \rightarrow C$ for a fixed constant $C > 0$.

3.2.1 Fixed Alternative

Assumption 1. *For independent random elements $\mathbf{Z}_X \sim \mathcal{P}_X$, $\mathbf{Z}_Y \sim \mathcal{P}_Y$, let us define $\mu_* \stackrel{\text{def}}{=} \mathbb{P}_* \left(\hat{\theta}(\mathbf{Z}_X) < \hat{\theta}(\mathbf{Z}_Y) \right)$ and $\mu \stackrel{\text{def}}{=} \mathbb{P}(\theta(\mathbf{Z}_X) < \theta(\mathbf{Z}_Y))$. Let us recall $\delta = \delta_T$ from (3.2). As $T \rightarrow \infty$, there exists some $\sqrt{1/T} \ll c_T < \delta_T/4$, such that $\mathbb{P} \left[|\mu_* - \mu| \leq \frac{\delta_T}{4} - c_T \right] \rightarrow 1$.*

Assumption 1 requires that, with high probability, the true signal order δ_T (hence $d_{tv}(\mathcal{P}_X, \mathcal{P}_Y)$ due to Proposition 2) should dominate the average approximation error incurred by estimating conditional probability using a classifier, which is denoted as $\mu_* - \mu$. The condition $\sqrt{1/T} \ll c_T < \delta_T/4$ is mild in that $\delta_T \gg \sqrt{1/T}$ under the fixed alternative. It requires that the estimated classifier can capture some signal from data other than purely statistical estimation error of order $\sqrt{1/T}$. Note that when δ_T is a fixed constant, a constant bound for the estimation error is sufficient to ensure both high power in the testing and the localization accuracy in the estimation (see Theorem 4 below). This highlights the robustness of our framework to estimation errors in the classifier, as it does not require the classifier to be consistently trained. Instead, we only require the estimated $\hat{\theta}(\cdot)$ to preserve the monotonicity of $\theta(\cdot)$ up to some tolerable error. This observation resonates with the assertions in Section 2.2 and is further underscored in Remark 2. In practice, the choice of the classifier could benefit from prior knowledge of the data structure. The following theorem ensures the consistency of our test under the fixed alternative setup.

Theorem 2. *Under H_1 , suppose Assumption 1 holds and $\sqrt{T}\delta_T \rightarrow \infty$. Then,*

$$\sup_{r \in [\gamma, 1-\gamma]} \left\{ \sqrt{T} \left(\hat{\Psi}(\lfloor Tr \rfloor) - \frac{1}{2} \right) \right\} \rightarrow \infty, \quad \text{in probability } \mathbb{P}_*.$$

3.2.2 Local Alternative

Assumption 2. *For random elements $\mathbf{Z}_1, \mathbf{Z}_2 \in E$ there exists $\zeta > 0$ such that the following holds true: (1) $\mathbb{E}_* \left| \mathbb{I} \left\{ \hat{\theta}(\mathbf{Z}_1) < \hat{\theta}(\mathbf{Z}_2) \right\} - \mathbb{I} \left\{ \theta(\mathbf{Z}_1) < \theta(\mathbf{Z}_2) \right\} \right| = O_{\mathbb{P}_*}(T^{-\zeta})$. Moreover, for $\mathbf{Z}_1 \sim \mathcal{P}_X$, $\mathbf{Z}_2 \sim \mathcal{P}_Y$ and $\mu_* = \mathbb{P}_* \left(\hat{\theta}(\mathbf{Z}_1) < \hat{\theta}(\mathbf{Z}_2) \right)$, $\mu = \mathbb{P}(\theta(\mathbf{Z}_1) < \theta(\mathbf{Z}_2))$, the following holds true: (2) $\mu_* - \mu = o_{\mathbb{P}_*}(T^{-1/2})$.*

Assumption 2(1) is slightly stronger than Assumption 1, and requires that $\hat{\theta}(\cdot)$ can consistently preserve the monotonicity of $\theta(\cdot)$. In the context of the local alternative hypothesis, where δ_T approaches zero as rapidly as $1/\sqrt{T}$, a more stringent condition in Assumption 2(2) is imposed on the average approximation error ($\mu_* - \mu$). Notably, the super consistency in Assumption 2(2) is applied to the expected rank monotonicity of conditional probabilities rather than

directly to the conditional probabilities. Similar assumptions have been recently utilized and verified in tests of independence (Theorem 7 in [Cai et al. \(2024\)](#)) and two-sample conditional distribution testing (Proposition 1 in [Hu and Lei \(2024\)](#)).

Theorem 3. *Suppose Assumption 2 is true. Under the local alternative such that $\sqrt{T}\delta_T \rightarrow C$, for some constant $C > 0$, then the following holds true:*

$$\left\{ \sqrt{T} \left(\widehat{\Psi}(\lfloor Tr \rfloor) - \frac{1}{2} \right) \right\}_{r \in [\gamma, 1-\gamma]} \overset{d}{\rightsquigarrow} \{ \Delta_G(r; \tau, \epsilon) + G_0(r) \}_{r \in [\gamma, 1-\gamma]}, \quad \text{in probability } \mathbb{P}_*,$$

where $G_0(\cdot)$ is defined in Theorem 1, and

$$\Delta_G(r; \tau, \epsilon) \stackrel{\text{def}}{=} \frac{C}{4} \begin{cases} (1 - \epsilon - \tau)/(1 - \epsilon - r) & \text{for } \gamma < r < \tau < 1 - \gamma, \\ (\tau - \epsilon)/(r - \epsilon) & \text{for } \gamma < \tau < r < 1 - \gamma. \end{cases}$$

3.3 Consistency of Change-point Estimator

The primary objective of this paper is to introduce a testing framework for a single change-point. Motivated by favorable localization performance observed in simulation studies, we establish the consistency result for estimating the change-point using $\widehat{R}_T = \operatorname{argmax}_{k \in \mathcal{I}_{cp}} \widehat{\Psi}(k)$.

Theorem 4. *Let $t_0 = \lfloor \tau T \rfloor$ be the true change-point. Under the fixed alternative $\delta_T \gg \sqrt{1/T}$, if Assumption 1 holds with $\sqrt{\log T/T} \ll c_T < \delta_T/4$, then*

$$\mathbb{P}_* \left[\left| \widehat{R}_T - t_0 \right| < C_L c_T^{-2} \log T \right] \geq 1 - o(1),$$

where $C_L > 0$ is a constant that only depends on the trimming parameters ϵ, η , and relative location of the true change-point τ .

Theorem 4 establishes the localization rate of the change-point estimator \widehat{R}_T . As an immediate consequence, we obtain its weak consistency, i.e., $\widehat{R}_T/T \rightarrow_p \tau$. In Theorem 4, the multiplicative order c_T^{-2} in the localization rate reflects the influence of classifier accuracy and the signal strength, where c_T quantifies the gap between classification performance and the signal strength δ_T in Assumption 1, and hence the total variation distance d_{tv} due to Proposition

2. The additional condition on $c_T \gg \sqrt{\log T/T}$ is mild because if $c_T = O(\sqrt{\log T/T})$, the localization rate becomes trivial. To gain more insights, if $\delta_T \asymp c_T$, the localization rate simplifies to $O_p(\delta_T^{-2} \log T) = O_p(d_{tv}^{-2} \log T)$, which according to Padilla et al. (2021) and Yu (2020), is minimax optimal up to a logarithmic factor in the univariate setting. Otherwise, if $c_T = o(\delta_T)$, the estimation effect of the classifier dominates the signal in the localization rate, which results in suboptimal performance of change-point estimation. In addition, Theorem (4) does not necessarily contradict the localization rate in Padilla et al. (2021) for multivariate data, where the signal is characterized by the (L_∞ -type) supremum distance between densities, whereas our approach utilizes the (L_1 -type) total variation distance. While it would be interesting to provide alternative lower bounds in this context, we defer this to future work.

4 Numerical Simulations

In this section, we examine the finite sample performance of our proposed method. The performance on high-dimensional Euclidean data is investigated in Section 4.1 whereas that on the non-Euclidean data using artificially constructed images from the CIFAR10 database (Krizhevsky et al., 2009) is presented in Section 4.2. Both R and Python code developed for `changeAUC` is available at <https://github.com/rohitkanrar/changeAUC>.

4.1 High Dimensional Euclidean Data

First, we examine the size and power performance of the proposed test in high-dimensional Euclidean data. We consider three classifiers, briefly summarized below:

- **Regularized Logistic:** (denoted by `Logis`) We apply the regularized logistic classifier with the LASSO penalty. R package `glmnet` is used (Friedman et al., 2010).
- **Fully-connected Neural Network:** (denoted by `Fnn`) We use a fully connected neural network with three hidden layers, ReLU activation and the binary cross-entropy loss.

Additionally, a LASSO penalty is enforced in each layer. Python framework `Tensorflow` is used (Abadi et al., 2016).

- **Random Forest:** (denoted by `Rf`) We employ a random forest classifier. `R` package `randomForest` (Liaw and Wiener, 2002) is used. Tuning parameters are set to default values as pre-fixed in the package.

For size performance, we consider the following data generating processes (DGP) with $T \in \{1000, 2000\}$ and $p \in \{10, 50, 200, 500, 1000\}$,

Standard Null: $\{\mathbf{Z}_t\}_{t=1}^T \stackrel{\text{iid}}{\sim} \mathcal{N}_p(\mathbf{0}_p, I_p)$;

Banded Null: $\{\mathbf{Z}_t\}_{t=1}^T \stackrel{\text{iid}}{\sim} \mathcal{N}_p(\mathbf{0}_p, \Sigma)$ with $\Sigma = (\sigma_{ij})_{i,j=1}^p$, $\sigma_{ij} = 0.8^{|i-j|}$;

Exponential Null: $\{\mathbf{Z}_{tj}\}_{t=1}^T \stackrel{\text{iid}}{\sim} \text{Exp}(1)$ for $j = 1, \dots, p$.

Table 2 presents the empirical rejection rates across 1000 replications at 5% significance level. The results demonstrate that all the considered classifiers successfully control the type-I error in all settings.

Table 2: Size performance of AUC over 1000 Monte Carlo replications, at 5% significance level(%).

	Standard Null			Banded Null			Exponential Null		
$(T, p) \backslash$ Classifier	Logis	Rf	Fnn	Logis	Rf	Fnn	Logis	Rf	Fnn
(1000,10)	3.6	2.5	4.4	3.6	2.5	3.9	3.6	4.7	4.5
(1000,50)	4.4	3.5	3.9	4.4	3.5	3.8	5.7	4.1	5.0
(1000,200)	4.4	4.1	5.4	4.4	4.1	4.5	5.2	5.1	5.0
(1000,500)	5.7	4.5	3.5	5.7	4.5	3.7	4.5	4.4	4.4
(1000,1000)	3.8	5.1	3.6	3.8	5.1	4.4	4.1	4.7	3.7
(2000,10)	3.8	3.1	2.8	3.8	3.1	4.8	4.4	3.7	4.6
(2000,50)	4.4	4.6	4.0	4.4	4.6	4.5	4.6	5.1	5.0
(2000,200)	5.2	4.7	3.5	5.2	4.7	5.0	5.2	4.7	4.5
(2000,500)	4.2	3.9	4.3	4.2	3.9	3.3	4.0	5.6	3.6
(2000,1000)	4.0	4.1	4.6	4.0	4.1	5.0	4.3	4.6	3.8

Next, we study the power performance in the high-dimensional setting. We fix the change-point location at $t_0 = \lfloor T/2 \rfloor$ with data length $T = 1000$, and data dimension $p \in \{500, 1000\}$, such that $\{\mathbf{Z}_t\}_{t=1}^{t_0} \stackrel{\text{iid}}{\sim} \mathcal{N}_p(\mathbf{0}_p, I_p)$. For the data after the change-point, the following data-generating processes are considered.

Dense Mean Change: $\{\mathbf{Z}_t\}_{t=t_0+1}^T \stackrel{\text{iid}}{\sim} \mathcal{N}_p(\boldsymbol{\mu}, I_p)$ with $\boldsymbol{\mu} = (\mu_i)_{i=1}^p$, $\mu_i = 2/\sqrt{\lfloor p/5 \rfloor}$ for $1 \leq i \leq \lfloor p/5 \rfloor$, and $\mu_i = 0$ for $\lfloor p/5 \rfloor + 1 \leq i \leq p$;

Sparse Mean Change: $\{\mathbf{Z}_t\}_{t=t_0+1}^T \stackrel{\text{iid}}{\sim} \mathcal{N}_p(\boldsymbol{\mu}, I_p)$ with $\boldsymbol{\mu} = (\mu_i)_{i=1}^p$, $\mu_i = 2/\sqrt{\lfloor p/100 \rfloor}$ for $1 \leq i \leq \lfloor p/100 \rfloor$, and $\mu_i = 0$ for $\lfloor p/100 \rfloor + 1 \leq i \leq p$;

Dense Cov Change: $\{\mathbf{Z}_t\}_{t=t_0+1}^T \stackrel{\text{iid}}{\sim} \mathcal{N}_p(\mathbf{0}_p, \Sigma)$ with $\Sigma = (\sigma_{ij})_{i,j=1}^p$, $\sigma_{ij} = 0.1\mathbb{I}(i \neq j)$;

Banded Cov Change: $\{\mathbf{Z}_t\}_{t=t_0+1}^T \stackrel{\text{iid}}{\sim} \mathcal{N}_p(\mathbf{0}_p, \Sigma)$ with $\Sigma = (\sigma_{ij})_{i,j=1}^p$, $\sigma_{ij} = 0.8^{|i-j|}$;

Dense Diag Cov Change: $\{\mathbf{Z}_t\}_{t=t_0+1}^T \stackrel{\text{iid}}{\sim} \mathcal{N}_p(\mathbf{0}_p, \Sigma)$, with $\Sigma = (\sigma_{ij})_{i,j=1}^p$, $\sigma_{ii} = 1 + 5/\sqrt{\lfloor p/5 \rfloor}$ for $1 \leq i \leq \lfloor p/5 \rfloor$, $\sigma_{ii} = 1$ for $\lfloor p/5 \rfloor + 1 \leq i \leq p$, and $\sigma_{ij} = 0$ for $i \neq j$;

Sparse Diag Cov Change: $\{\mathbf{Z}_t\}_{t=t_0+1}^T \stackrel{\text{iid}}{\sim} \mathcal{N}_p(\mathbf{0}_p, \Sigma)$, with $\Sigma = (\sigma_{ij})$, where $\sigma_{ii} = 1 + 5/\sqrt{\lfloor p/100 \rfloor}$ for $1 \leq i \leq \lfloor p/100 \rfloor$, $\sigma_{ii} = 1$ for $\lfloor p/100 \rfloor + 1 \leq i \leq p$, and $\sigma_{ij} = 0$ for $i \neq j$;

Dense Distribution Change: $\{\mathbf{Z}_{tj}\}_{t=t_0+1}^T \stackrel{\text{iid}}{\sim} \text{Exp}(1)-1$ for $j = 1, \dots, \lfloor p/5 \rfloor$ and $\{\mathbf{Z}_{tj}\}_{t=t_0+1}^T \stackrel{\text{iid}}{\sim} \mathcal{N}_1(0, 1)$ for $j = \lfloor p/5 \rfloor + 1, \dots, p$;

Sparse Distribution Change: $\{\mathbf{Z}_{tj}\}_{t=t_0+1}^T \stackrel{\text{iid}}{\sim} \text{Exp}(1)-1$ for $j = 1, \dots, \lfloor p/100 \rfloor$ and $\{\mathbf{Z}_{tj}\}_{t=t_0+1}^T \stackrel{\text{iid}}{\sim} \mathcal{N}_1(0, 1)$ for $j = \lfloor p/100 \rfloor + 1, \dots, p$.

Note that for the distributional changes, the first- and second-order moments of the underlying distributions remain the same before and after the change-point.

In addition to the proposed methods, we consider the following four competitors among many existing tests for detecting change-points in high-dimensional data.

- A graph-based method `gseg` proposed by [Chen and Zhang \(2015\)](#) and [Chu and Chen \(2019\)](#), and is implemented by the `gSeg` package in R. Here, the graph is constructed using the minimal spanning tree, and two edge-count scan statistics are considered: weighted (`gseg_wei`) and max-type (`gseg_max`).
- A generalized energy distance-based method proposed by [Chakraborty and Zhang \(2021\)](#) (denoted as `Hddc`). The default distance metric $\gamma(z, z') = \|z - z'\|_1^{1/2}$ is utilized to calculate the interpoint distance.
- A density-ratio based method applied on sliding windows, proposed by [Wang et al. \(2023\)](#) (denoted as `NODE`). Deep neural network with default configuration is employed to estimate the density ratios.
- A two-step nonparametric likelihood with the random forest-based method proposed by [Londschien et al. \(2023\)](#) (denoted as `changeforest`). All tuning parameters are fixed to the default values suggested by the authors.

We first assess the computational efficiency of the proposed methods in comparison to existing ones. To illustrate the idea, we use a 16-core AMD EPYC 7542 CPU with 32 GB RAM for all methods except for `Fnn`, which is performed using a single-core Intel Xeon 6226R CPU with a single NVIDIA Tesla V100 GPU. Data generation follows the “Dense Mean” setup, with performance under other settings being similar and thus omitted.

Table 3 presents the average computation time for all five methods over 1000 replications, with standard deviations shown in parentheses. It is evident that our proposed methods `Logis`, `Fnn` and `Rf`, along with `gseg`, exhibit considerable speed, making them feasible for implementation within a reasonable time. However, owing to the recursive calculation of U -statistics, `Hddc` is notably sluggish, making it nearly impractical for implementation on personal laptops. Although both `changeforest` and `Rf` apply the random forest, the former takes more time due to permutation-based testing procedure and two-step search. Note that `NODE` also trains a

deeper neural network like our method **Fnn**. The former one is a sliding window-based search procedure, which explains its high computational cost.

Table 3: Average computation time (in seconds) across 1000 replications from the “Dense Mean Change” setup with $T = 1000$, with standard deviation in the parenthesis below.

p	gseg	Hddc	NODE	changeforest	Logis	Fnn	Rf
500	1.473	$> 10^4$	235.1	4.258	0.101	2.539	0.697
	(0.013)	($> 3 \times 10^4$)	(0.38)	(0.17)	(0.031)	(0.351)	(0.013)
1000	1.476	$> 6 \times 10^4$	553.2	8.751	0.122	2.592	1.3
	(0.012)	($> 8 \times 10^4$)	(8.5)	(0.05)	(0.036)	(0.338)	(0.020)

To further examine the effectiveness of these approaches, following [Chakraborty and Zhang \(2021\)](#), we use Adjusted Rand Index (ARI) ([Morey and Agresti, 1984](#)) to measure the accuracy of the estimated change-points, which is commonly used to evaluate clustering algorithms. In the context of change-point problems, an ARI close to zero indicates a larger disparity between the estimated and true change-points or detects a change-point without any actual change. Conversely, an ARI of one indicates a perfect estimation of true change-points. We fix ARI as zero if no significant change-point is detected.

The empirical performance from 500 Monte Carlo repetitions is depicted in Figure 1 through boxplots. We list our findings as follows. 1) Our proposed methods (including **Logis**, **Fnn** and **Rf**) together with **Hddc** and **changeforest** are powerful in detecting both dense and sparse mean changes. 2) The **gseg** methods lose power in distributional changes, while **Hddc** worsens when changes occur in dense or banded covariance matrices. This corroborates the findings in [Chakraborty and Zhang \(2021\)](#). 3) **NODE** does not perform well in any setup, and we conjecture this is due to the curse of high dimensionality. 4) **changeforest** and **Rf** demonstrate competitive performance across all types of changes, with **Rf** showing a slight advantage in the “Dense Diag Cov Change” setup. 5) Finally, we mention that the performance of our methods is varied; it

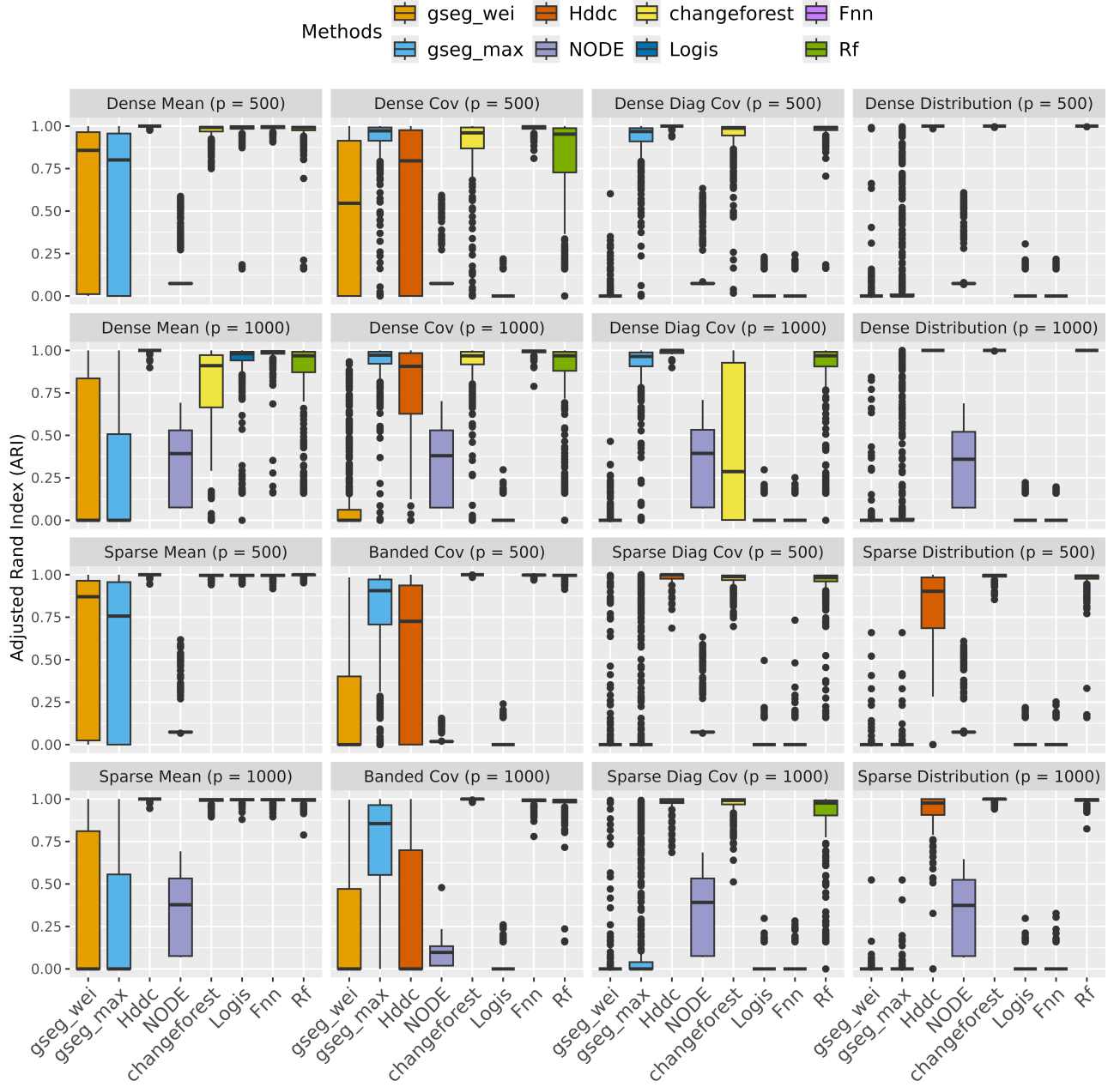


Figure 1: Boxplots of ARI values across 500 repetitions. The first and third rows correspond to dimension $p = 500$, and the second and fourth rows to dimension $p = 1000$, respectively. The columns represent different DGPs under consideration. Each boxplot contains eight methods considered/compared in this paper.

depends on the chosen classifiers, especially when changes occur in higher-order moments or distributions. In particular, we note that **Logis** performs well in detecting mean changes only and loses power in other setups. As for **Fnn**, it is most powerful in detecting changes in dense or banded covariances, while its performance deteriorates in other settings. We conjecture that this is due to the necessity of certain dependence among the data dimensions for a neural network to train effectively. On the other hand, the performance of **Rf** is quite robust in all settings. In summary, if certain prior knowledge of the data is available, our proposed framework can work effectively when paired with a suitable classification algorithm.

4.2 Non-Euclidean CIFAR10 Data

In this section, we examine the size and power performance of the proposed method in high-dimensional non-Euclidean data. In particular, we detect change-points in artificially constructed sequences of images of various animals (dog, cat, deer, horse, etc.) from the CIFAR10 database (Krizhevsky et al., 2009), see Figure 2 for visual illustration. Since the ground truth is known, we can accurately assess both the size and power of the method. To this end, we apply two pre-trained deep convolutional neural network (CNN) classifiers.

- **vgg16, vgg19:** Simonyan and Zisserman (2014) propose a deep CNN classifier with 16-19 hidden layers and a small 3-by-3 convolution filter. In the machine-learning community, it is a common practice to use pre-trained deep CNN classifiers such as **vgg16** and **vgg19** to classify images in new datasets. Here, we adopt the pre-trained weight ‘imagenet’ (Deng et al., 2009), which is default in **Tensorflow**.



Figure 2: RGB 32-by-32 images of a Cat, Deer, Dog, and Horse from CIFAR10 Database.

To evaluate the size performance, we randomly sample 1000 images of deer and dogs in two separate sequences of images. As for the alternative, we randomly choose 500 images of two different animal categories for each replication and arrange them so that the first 500 images correspond to one animal and the next 500 to the other. Hence, the true change-point is located at $t_0 = 500$. We consider three choices for such pairs: (Cat \rightarrow Dog), (Deer \rightarrow Dog) and (Dog \rightarrow Horse).

Out of all the methods considered, we consider two graph based methods **gseg_wei** and **gseg_max**, and the **changeforest** method for comparison. Here, we perform a row-major vectorization of the three-dimensional tensor to apply **changeforest** on image data. The proposed method based on AUC is denoted as **vgg16** and **vgg19**. The default ‘imagenet’ embeddings are frozen to train classifiers, and only the last layer of the neural network is modified during back-propagation. A single feed-forward layer with 512 neurons is added on top of the embeddings. To further demonstrate the robustness of our AUC-based statistic, we additionally include a baseline algorithm where the classical CUSUM statistic is computed using the one-dimensional embedding, denoted as **vgg16_cusum** and **vgg19_cusum**. Appendix ?? includes more details on this statistic and its implementation.

Table 4: Size and Power performance of all methods: the first two rows correspond to the size, and the last three rows correspond to average ARI values.

	Cases	<code>gseg.wei</code>	<code>gseg.max</code>	<code>changeforest</code>	<code>vgg16</code> <code>cusum</code>	<code>vgg19</code> <code>cusum</code>	<code>vgg16</code>	<code>vgg19</code>
Size	Deer	4.3%	4.9%	6%	0%	0%	4%	3.8%
	Dog	4.2%	4.6%	5%	0%	0%	3.4%	4%
ARI	Cat \rightarrow Dog	0.378	0.289	0.952	0.002	0	0.965	0.963
	Deer \rightarrow Dog	0.976	0.976	0.992	1	1	0.997	0.996
	Deer \rightarrow Horse	0.970	0.968	0.992	1	1	0.994	0.993

Table 4 summarizes the performance of all methods. The first two rows consist of the empirical rejection rate at the significance level 5% when no change-point exists, and the last three rows enlist average ARI across 500 replications when there is a change-point. We summarize our finding as follows. 1) The testing framework of `gseg` using permutation-based p-values successfully controls the type-I error, and they can perform well when the change type is relatively easy to detect but fail in the most challenging scenario (Cat \rightarrow Dog). 2) The proposed methods `vgg16` and `vgg19`, along with `changeforest` perform favorably in all scenarios, with `vgg` methods showing a slight advantage in the case (Cat \rightarrow Dog). 3) For the CUSUM-based testing procedure using direct output probabilities of `vgg` classifiers, we observe that they fail to control the Type-I error, and has no power in the case of (Cat \rightarrow Dog). We conjecture that this issue arises from the estimation effect of the classifier, which disrupts the use of classical CUSUM pivotal limiting distribution. This further corroborates the robustness of the AUC-based framework.

5 Real Data applications

In this section, we present two real data applications and compare the performance of our proposed method with other methods considered in Section 4.

5.1 US Stock Market during the Great Recession

Detecting shifts in financial markets is crucial for policymakers and investors. In this section, we apply the proposed methods to the NYSE and NASDAQ stock data from 2005 to 2010. Our study builds upon [Chakraborty and Zhang \(2021\)](#) where stock price changes of 72 companies under the “Consumer Defensive” sector are analyzed. Here, we expand our focus to a larger dataset comprising daily log returns of 289 companies across the “Healthcare”, “Consumer Defensive,” and “Utilities” sectors from January 2005 to December 2010. These sectors were identified as “Recession-Proof Industries” during the “Great Recession” from December 2007 to June 2009, during which the US Federal Government implemented fiscal stimulus packages to stabilize the economy. Table 5 outlines the estimated change-points using `gseg` type methods, `Hddc`, `NODE`, `changeforest` and `Rf`. Each method is embedded into the Seeded Binary Segmentation ([Kovács et al., 2023](#)) algorithm to estimate multiple change-points. From the table, we find that estimated change-points using our method `Rf` are aligned with important historical dates during the recession. For example, in early August 2007* (identified by 07-25-2007), the market experienced a liquidity crisis, and in September 2008 (identified by 09-09-2008) the international banking crisis happened caused by the bankruptcy of “Lehman Brothers” ([Wiggins et al., 2014](#)). However, the change-points reported by the `gseg` methods differ significantly. Given that for stock price data, changes in daily log returns typically manifest in higher-order moments beyond the mean, we conjecture that this discrepancy is due to their impaired performance in estimating distributional changes, as indicated in Section 4.1. The change-points detected by `Hddc` are close to ours, albeit a miss in 2008; while `changeforest` reports no change in 2007. Finally, we note `NODE` fails to detect any changes.

*<http://news.bbc.co.uk/1/hi/business/7521250.stm>

Table 5: Estimated change-points (in MM-DD format) of US Stock Data

Years	2006	2007	2008	2009
<code>gseg_wei</code>	11-29	02-12	05-30	12-02
<code>gseg_max</code>	12-18	02-12	05-30	11-19
<code>Hddc</code>	08-09	07-25	-	07-13
<code>NODE</code>	-	-	-	-
<code>changeforest</code>	08-10	-	01-02	06-04
<code>Rf</code>	08-09	07-25	09-09	08-07

5.2 New York Taxi Trips during the COVID-19 Pandemic

The COVID-19 Pandemic significantly impacted New York State, particularly in early 2020. The state, especially New York City (NYC), became an epicenter for the virus, with strict lockdown measures implemented to curb the spread. This study investigates the impact of several lockdowns enforced in NYC during the COVID-19 pandemic. We collect For-Hire Vehicle (FHV) Trip records during 2018 and 2022 from the NYC Taxi and Limousine Commission (TLC) Trip Record Database.[†] These records contain crucial details such as pickup and drop-off times, drop-off location, trip distances, and other information. To harness the geographical insights within the dataset, we employed the name of the borough associated with each drop-off point to generate daily areal heat maps. These heat maps visually depict the estimated spatial density of drop-off counts; see Figure 3 for six such heat-maps. In Chu and Chen (2019), the same data source (during different time horizons and different types of taxi) is analyzed by summarizing the information on the number of taxi drop-offs into a 30 by 30 matrix.

Table 6 showcases the estimated change-points obtained through our method with the `vgg16` classifier and `gseg` type methods. Notably, the change-points identified by both methods closely align with each other except for 2021. These significant shifts correspond to events such as the

[†]<https://www.nyc.gov/site/tlc/about/tlc-trip-record-data.page>

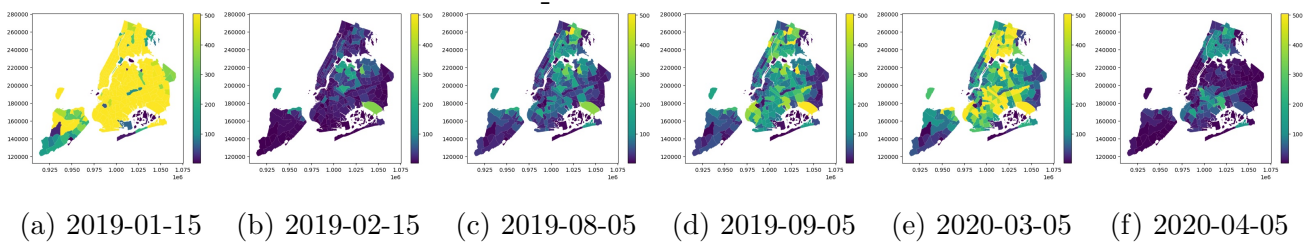


Figure 3: Areal heatmaps of daily taxi trip counts in New York City on six different days before and during the COVID-19 pandemic.

Table 6: Estimated change-points (in MM-DD format) of New York taxi data

Years	2018	2019	2020	2021	2022
<code>gseg_wei</code>	-	01-31, 10-01	03-16, 08-01	07-01	04-01
<code>gseg_max</code>	-	01-31, 10-01	03-16, 08-01	07-01	04-01
<code>changeforest</code>	-	04-01	06-25	09-01	-
<code>vgg16</code>	-	01-31, 08-31	03-17, 11-29	10-31	04-03

2019 North American cold wave (2019-01-31), the potential impact of summer vacation (2019-08-31), and the implementation of NYC’s first lockdown (2020-03-17). For instance, Figure 3a and 3b depict the areal heat maps on January 15, 2019 (before the heatwave) and February 15, 2019 (after the heatwave), respectively, revealing a noteworthy decrease in taxi usage. Subsequently, areal heat maps in Figure 3c and 3d illustrate an increasing effect on taxi usage following the end of summer vacation. Additionally, Figure 3e and 3f present the areal heat maps on March 5, 2020 (before the lockdown) and April 5, 2020 (after the lockdown), respectively, indicating a significant decline in taxi usage. However, we find the estimated change-points by `changeforest` differ significantly from the other two methods.

6 Discussion

In this paper, we propose a novel framework for offline change-point detection based on the AUC of classifiers. Despite the vast literature on change-point detection, our approach stands out in four key aspects. First, our method is entirely nonparametric, as it does not impose any parametric assumptions on the data distribution or the structure of distributional changes. Second, by leveraging the success of classifiers, the proposed framework is widely applicable to diverse data dimensions and types. Third, by selecting an appropriate classifier, prior information can be integrated to enhance the test power. Last but not least, with suitable sample splitting and trimming, the test statistic converges to the supremum of a pivotal Gaussian process, which is independent of the choice of classifier and thus can be easily implemented. Another key advantage of our proposed method is that it can incorporate weakly trained and fine-tuned pre-trained classifiers. Rank-sum comparison embedded in the AUC makes this integration robust to estimation error in classification probabilities.

To conclude, we mention a few directions that warrant future investigation. First, it should be noted that the real data analysis in Section 5 may exhibit temporal dependence. Extending the proposed method to accommodate weakly dependent time series would be an intriguing endeavor. Second, it may be feasible to reduce the computational burden by drawing inspiration from [Londschien et al. \(2023\)](#). Instead of computing the AUC for all potential change-points, it could be computed for initial points, such as the quartiles of the sequence, followed by an extensive search in proximity to the initial candidate change-point that yields the highest AUC. However, exploring the theoretical properties of such a two-stage approach may be challenging. Third, the current setting is unsupervised and, therefore, requires certain sample splitting and trimming; it would be interesting to investigate the asymptotic properties of the test statistic under the supervised setting, as in [Li et al. \(2024\)](#). Fourth, it will be useful to extend our framework to the online setting. We leave these directions to future research.

References

- Abadi, M., Agarwal, A., Barham, P., Brevdo, E., Chen, Z., Citro, C., Corrado, G.S., Davis, A., Dean, J., Devin, M., et al. (2016). “TensorFlow: Large-scale machine learning on heterogeneous systems.” *arXiv preprint arXiv:1603.04467*.
- Anastasiou, A. and Fryzlewicz, P. (2022). “Detecting multiple generalized change-points by isolating single ones.” *Metrika*, **85(2)**, 141–174.
- Andrews, D.W. (1993). “Tests for parameter instability and structural change with unknown change point.” *Econometrica*, pages 821–856.
- Arlot, S., Celisse, A., and Harchaoui, Z. (2019). “A kernel multiple change-point algorithm via model selection.” *Journal of Machine Learning Research*, **20(162)**, 1–56.
- Atto, A.M., Bovolo, F., and Bruzzone, L. (2021). *Change Detection and Image Time Series Analysis 2: Supervised Methods*. John Wiley & Sons.
- Aue, A. and Horváth, L. (2013). “Structural breaks in time series.” *Journal of Time Series Analysis*, **34(1)**, 1–16.
- Aue, A., Rice, G., and Sönmez, O. (2018). “Detecting and dating structural breaks in functional data without dimension reduction.” *Journal of the Royal Statistical Society Series B: Statistical Methodology*, **80(3)**, 509–529.
- Avanesov, V. and Buzun, N. (2018). “Change-point detection in high-dimensional covariance structure.” *Electronic Journal of Statistics*, **12(2)**, 3254 – 3294.
- Berkes, I., Gabrys, R., Horváth, L., and Kokoszka, P. (2009). “Detecting changes in the mean of functional observations.” *Journal of the Royal Statistical Society Series B: Statistical Methodology*, **71(5)**, 927–946.

- Cai, Z., Lei, J., and Roeder, K. (2022). “Model-free prediction test with application to genomics data.” *Proceedings of the National Academy of Sciences*, **119(34)**, e2205518119.
- Cai, Z., Lei, J., and Roeder, K. (2024). “Asymptotic distribution-free independence test for high-dimension data.” *Journal of the American Statistical Association*, **119(547)**, 1794–1804.
- Chakraborty, S. and Zhang, X. (2021). “High-dimensional change-point detection using generalized homogeneity metrics.” *arXiv preprint arXiv:2105.08976*.
- Chakravarti, P., Kuusela, M., Lei, J., and Wasserman, L. (2023). “Model-independent detection of new physics signals using interpretable semisupervised classifier tests.” *The Annals of Applied Statistics*, **17(4)**, 2759–2795.
- Chen, H. and Zhang, N. (2015). “Graph-based change-point detection.” *The Annals of Statistics*, **43(1)**, 139 – 176.
- Chen, J. and Gupta, A.K. (2012). *Parametric statistical change point analysis: with applications to genetics, medicine, and finance*. Springer.
- Cho, H. and Fryzlewicz, P. (2015). “Multiple-change-point detection for high dimensional time series via sparsified binary segmentation.” *Journal of the Royal Statistical Society Series B: Statistical Methodology*, **77(2)**, 475–507.
- Chu, L. and Chen, H. (2019). “Asymptotic distribution-free change-point detection for multivariate and non-Euclidean data.” *The Annals of Statistics*, **47(1)**, 382 – 414.
- Deng, J., Dong, W., Socher, R., Li, L.J., Li, K., and Fei-Fei, L. (2009). “Imagenet: A large-scale hierarchical image database.” In “2009 IEEE conference on computer vision and pattern recognition,” pages 248–255. Ieee.
- Detle, H., Pan, G., and Yang, Q. (2022). “Estimating a change point in a sequence of very high-

- dimensional covariance matrices.” *Journal of the American Statistical Association*, **117**(537), 444–454.
- Dubey, P. and Müller, H.G. (2020). “Fréchet change-point detection.” *The Annals of Statistics*, **48**(6), 3312–3335.
- Dubey, P. and Zheng, M. (2023). “Change point detection for random objects using distance profiles.” *arXiv preprint arXiv:2311.16025*.
- Enikeeva, F. and Harchaoui, Z. (2019). “High-dimensional change-point detection under sparse alternatives.” *The Annals of Statistics*, **47**(4), 2051 – 2079.
- Fawcett, T. (2006). “An introduction to ROC analysis.” *Pattern Recognition Letters*, **27**(8), 861–874.
- Friedman, J., Hastie, T., and Tibshirani, R. (2010). “Regularization paths for generalized linear models via coordinate descent.” *Journal of Statistical Software*, **33**(1), 1–22.
- Fryzlewicz, P. (2014). “Wild binary segmentation for multiple change-point detection.” *The Annals of Statistics*, **42**(6), 2243 – 2281.
- Gao, H., Wang, R., and Shao, X. (2023). “Dimension-agnostic change point detection.” *arXiv preprint arXiv:2303.10808*.
- Harchaoui, Z. and Cappé, O. (2007). “Retrospective mutiple change-point estimation with kernels.” *2007 IEEE/SP 14th Workshop on Statistical Signal Processing*, pages 768–772.
- Hu, X. and Lei, J. (2024). “A two-sample conditional distribution test using conformal prediction and weighted rank sum.” *Journal of the American Statistical Association*, **119**(546), 1136–1154.
- Jiang, F., Zhu, C., and Shao, X. (2024). “Two-sample and change-point inference for non-Euclidean valued time series.” *Electronic Journal of Statistics*, **18**(1), 848 – 894.

- Jiao, S., Frostig, R.D., and Ombao, H. (2023). “Break point detection for functional covariance.” *Scandinavian Journal of Statistics*, **50(2)**, 477–512.
- Jirak, M. (2015). “Uniform change point tests in high dimension.” *The Annals of Statistics*, **43(6)**, 2451 – 2483.
- Kaul, A., Jandhyala, V.K., and Fotopoulos, S.B. (2019). “An efficient two step algorithm for high dimensional change point regression models without grid search.” *Journal of Machine Learning Research*, **20**, 1–40.
- Kawahara, Y. and Sugiyama, M. (2012). “Sequential change-point detection based on direct density-ratio estimation.” *Statistical Analysis and Data Mining: The ASA Data Science Journal*, **5(2)**, 114–127.
- Kim, I., Lee, A.B., and Lei, J. (2019). “Global and local two-sample tests via regression.” *Electronic Journal of Statistics*, **13**, 5253–5305.
- Kim, I., Ramdas, A., Singh, A., and Wasserman, L. (2021). “Classification accuracy as a proxy for two sample testing.” *The Annals of Statistics*, **49(1)**, 411–434.
- Kirchler, M., Khorasani, S., Kloft, M., and Lippert, C. (2020). “Two-sample testing using deep learning.” In S. Chiappa and R. Calandra, editors, “Proceedings of the Twenty Third International Conference on Artificial Intelligence and Statistics,” volume 108 of *Proceedings of Machine Learning Research*, pages 1387–1398. PMLR.
- Kovács, S., Bühlmann, P., Li, H., and Munk, A. (2023). “Seeded binary segmentation: a general methodology for fast and optimal changepoint detection.” *Biometrika*, **110(1)**, 249–256.
- Krizhevsky, A., Nair, V., and Hinton, G. (2009). “CIFAR-10 (canadian institute for advanced research).”

- Labuzzetta, C.J. and Zhu, Z. (2024). “Mapping conservation practices via deep learning: Improving performance via hillshade imagery, sampling design, and centerline dice loss.” *Statistics and Data Science in Imaging*, **1(1)**, 2401756.
- Lee, J., Xie, Y., and Cheng, X. (2023). “Training neural networks for sequential change-point detection.” In “IEEE ICASSP 2023,” pages 1–5. IEEE.
- Li, J., Fearnhead, P., Fryzlewicz, P., and Wang, T. (2024). “Automatic change-point detection in time series via deep learning.” *Journal of the Royal Statistical Society Series B: Statistical Methodology*, **86(2)**, 273–285.
- Li, Y.N., Li, D., and Fryzlewicz, P. (2023). “Detection of multiple structural breaks in large covariance matrices.” *Journal of Business & Economic Statistics*, **41(3)**, 846–861.
- Liaw, A. and Wiener, M. (2002). “Classification and regression by randomforest.” *R News*, **2(3)**, 18–22.
- Liu, B., Zhou, C., Zhang, X., and Liu, Y. (2020). “A unified data-adaptive framework for high dimensional change point detection.” *Journal of the Royal Statistical Society Series B: Statistical Methodology*, **82(4)**, 933–963.
- Liu, S., Yamada, M., Collier, N., and Sugiyama, M. (2013). “Change-point detection in time-series data by relative density-ratio estimation.” *Neural Networks*, **43**, 72–83.
- Londschien, M., Bühlmann, P., and Kovács, S. (2023). “Random forests for change point detection.” *Journal of Machine Learning Research*, **24(216)**, 1–45.
- Lopez-Paz, D. and Oquab, M. (2016). “Revisiting classifier two-sample tests.” *International Conference on Learning Representations, arXiv preprint arXiv:1610.06545*.
- Matteson, D.S. and James, N.A. (2014). “A nonparametric approach for multiple change point

- analysis of multivariate data.” *Journal of the American Statistical Association*, **109**(505), 334–345.
- Morey, L.C. and Agresti, A. (1984). “The measurement of classification agreement: An adjustment to the Rand statistic for chance agreement.” *Educational and Psychological Measurement*, **44**, 33 – 37.
- Padilla, O.H.M., Yu, Y., Wang, D., and Rinaldo, A. (2021). “Optimal nonparametric multivariate change point detection and localization.” *IEEE Transactions on Information Theory*, **68**(3), 1922–1944.
- Page, E.S. (1954). “Continuous inspection schemes.” *Biometrika*, **41**(1/2), 100–115.
- Simonyan, K. and Zisserman, A. (2014). “Very deep convolutional networks for large-scale image recognition.” *arXiv preprint arXiv:1409.1556*.
- Steland, A. (2019). “Testing and estimating change-points in the covariance matrix of a high-dimensional time series.” *Journal of Multivariate Analysis*, **177**, 104582.
- Truong, C., Oudre, L., and Vayatis, N. (2020). “Selective review of offline change point detection methods.” *Signal Processing*, **167**, 107299.
- Vaart, A.v.d. and Wellner, J.A. (2023). “Empirical processes.” In “Weak Convergence and Empirical Processes: With Applications to Statistics,” pages 127–384. Springer.
- Wang, R., Zhu, C., Volgushev, S., and Shao, X. (2022). “Inference for change points in high-dimensional data via selfnormalization.” *The Annals of Statistics*, **50**(2), 781–806.
- Wang, T. and Samworth, R.J. (2018). “High dimensional change point estimation via sparse projection.” *Journal of the Royal Statistical Society Series B: Statistical Methodology*, **80**(1), 57–83.

- Wang, X., Borsoi, R.A., Richard, C., and Chen, J. (2023). “Change point detection with neural online density-ratio estimator.” In “ICASSP 2023-2023 IEEE International Conference on Acoustics, Speech and Signal Processing (ICASSP),” pages 1–5. IEEE.
- Wiggins, R., Piontek, T., and Metrick, A. (2014). “The lehman brothers bankruptcy a: overview.” *Yale program on financial stability case study*.
- Yu, M. and Chen, X. (2020). “Finite sample change point inference and identification for high-dimensional mean vectors.” *Journal of the Royal Statistical Society Series B: Statistical Methodology*, **83(2)**, 247–270.
- Yu, Y. (2020). “A review on minimax rates in change point detection and localisation.” *arXiv preprint arXiv:2011.01857*.
- Zhao, Z., Jiang, F., and Shao, X. (2022). “Segmenting time series via self-normalisation.” *Journal of the Royal Statistical Society Series B: Statistical Methodology*, **84(5)**, 1699–1725.
- Zou, C., Yin, G., Feng, L., and Wang, Z. (2014). “Nonparametric maximum likelihood approach to multiple change-point problems.” *The Annals of Statistics*, **42(3)**, 970 – 1002.